The "Sausage" and "Toothbrush" clusters of galaxies and the prospects of LOFAR observations of clusters of galaxies

Astron. Nachr. / AN **334**, No. 4/5, 333 – 337 (2013) / **DOI** 10.1002/asna.201211847

The "Sausage" and "Toothbrush" clusters of galaxies and the prospects of LOFAR observations of clusters of galaxies

H. Röttgering[1,⋆], R. van Weeren[2], M. Brüggen[3], J. Croston[4], M. Hoeft[5], G. Ogrean[3], P. Barthel[6], P. Best[7], A. Bonafede[3], G. Brunetti[8], R. Cassano[8], K. Chyży[9], J. Conway[10], F. De Gasperin[3], C. Ferrari[11], G. Heald[12], N. Jackson[14], M. Jarvis[13], M. Lehnert[15], G. Macario[11], G. Miley[1], E. Orrú[12], R. Pizzo[12], D. Rafferty[1], A. Stroe[1], C. Tasse[16], S. van der Tol[1], G. White[17], M. Wise[12], and **on behalf of the LOFAR collaboration**

[1] Sterrewacht Leiden, PO Box 9513, 2300 RA Leiden, The Netherlands
[2] Smithsonian Astrophysical Observatory, 60 Garden Street, Cambridge, MA 02138, USA
[3] Hamburger Sternwarte, Universität Hamburg, Gojenbergsweg 112, 21029 Hamburg, Germany
[4] School of Physics and Astronomy, University of Southampton, Southampton SO17 1BJ, UK
[5] Thüringer Landessternwarte, Tautenburg, Germany
[6] Kapteyn Instituut, Landleven 12, 9747 AD Groningen, The Netherlands
[7] Royal Observatory, Blackford Hill, Edinburgh EH9 3HJ, UK
[8] INAF, Istituto di Radioastronomia, Via P Gobetti 101, IT 40129, Bologna, Italy
[9] Obserwatorium Astronomiczne Uniwersytetu Jagiellońskiego, ul. Orla 171 30-244 Kraków, Poland
[10] Chalmers University of Technology, Onsala Space Observatory, SE 439 92 Onsala, Sweden
[11] Laboratoire Lagrange, UMR7293, Université de Nice Sophia-Antipolis, CNRS, Observatoire de la Côte d'Azur, 06300 Nice, France
[12] ASTRON, PO Box 2, 7990 AA Dwingeloo, The Netherlands
[13] Department of Physics, University of Oxford Astrophysics, Keble Road, Oxford OX1 3RH, UK; Department of Physics, University of the Western Cape, Private Bag X17, Bellville 7535, South Africa
[14] Jodrell Bank Centre for Astrophysics, University of Manchester, Turing Building, Oxford Road, Manchester M13 9PL, UK
[15] Observatoire de Paris, 5 Place Jules Janssen, 92195 Meudon, France
[16] Rhodes University, P.O. Box 94 Grahamstown 6140, South Africa
[17] Department of Physics and Astronomy, The Open University, Milton Keynes, MK7 6AA, UK; Space Science and Technology Department, STFC Rutherford Appleton Laboratory, Chilton, OX11 0QX, UK

Received 2012 Nov 9, accepted 2012 Nov 24
Published online 2013 May 2

Key words galaxies: clusters: general – galaxies: clusters: individual(CIZA J2242.8+5301, 1RXS J0603.3+4214) – telescopes

LOFAR, the Low Frequency Radio Array, is a new pan-European radio telescope that is almost fully operational. One of its main drivers is to make deep images of the low frequency radio sky. To be able to do this a number of challenges need to be addressed. These include the high data rates, removal of radio frequency interference, calibration of the beams and correcting for the corrupting influence of the ionosphere. One of the key science goals is to study merger shocks, particle acceleration mechanisms and the structure of magnetic fields in nearby and distant merging clusters. Recent studies with the GMRT and WSRT radio telescopes of the "Sausage" and the "Toothbrush" clusters have given a very good demonstration of the power of radio observations to study merging clusters. Recently we discovered that both clusters contain relic and halo sources, large diffuse regions of radio emission not associated with individual galaxies. The 2 Mpc northern relic in the Sausage cluster displays highly aligned magnetic fields and and exhibits a strong spectral index gradient that is a consequence of cooling of the synchrotron emitting particles in the post-shock region. We have argued that these observations provide strong evidence that shocks in merging clusters are capable of accelerating particles. For the Toothbrush cluster we observe a puzzling linear relic that extends over 2 Mpc. The proposed scenario is that a triple-merger can lead to such a structure. With LOFAR's sensitivity it will not only be possible to trace much weaker shocks, but also to study those shocks due to merging clusters up to redshifts of at least one.

1 Introduction

LOFAR, the Low Frequency Array, is a next-generation radio telescope. Its novel design with 40 antenna stations spread over the northern parts of the Netherlands and 8 over

⋆ Corresponding author: rottgering@strw.leidenuniv.nl

northern Europe will open up the radio sky for observations at frequencies between 15 and 240 MHz (corresponding to wavelengths of 20 to 1.2 m). The resulting high sensitivity and angular resolution, coupled with its large field of view, flexible spectroscopic and high time resolution capabilities will enable us for the first time to deeply map the entire northern sky at the lowest radio frequencies accessible from the ground.

Galaxy clusters are unique laboratories to study some of the most fundamental questions in astrophysics, related to the formation and evolution of galaxies, the physics of particle acceleration, the growth of large-scale structure, and cosmology. Using LOFAR's unique diagnostic tools a coherent study of clusters of galaxies over the entire history of the universe since the formation of the first proto-clusters will be carried out. Detailed observations of diffuse radio emission from nearby clusters will delineate how cluster merger shocks and AGN feedback shape the physical characteristics of the thermal and non-thermal cluster gas. The LOFAR surveys have the potential to detect thousands of these systems up to redshifts $z = 1$–2, i.e. at the epoch when the first bound clusters appeared. Studies of the associated shock waves produced by cluster mergers will constrain models of the formation of galaxy clusters and and measure their magnetic fields and relativistic particle content.

In this contribution we will first discuss the status of the LOFAR project. In particular, emphasis will be given to the challenges that will be faced to be able to make deep, high quality images of the low frequency sky. Very briefly, some preliminary LOFAR results are discussed. In the second part of this contribution we we will present our recent results on radio and X-ray observations on two spectacular radio shocks of 2 Mpc in size in two clusters that we nicknamed the "Sausage" and the "Toothbrush" cluster.

2 LOFAR

LOFAR's revolutionary design makes use of phased array technology. This replaces the traditional and expensive mechanical dishes with a combination of simple receivers and modern computing equipment. LOFAR has two types of antennas, one optimized for the 30–80 MHz range (see Fig. 1) and one for the 115–200 MHz range. The antennas are grouped together in stations the size of soccer fields. The signals from the antennas are digitized and combined with appropriate phase delays to form beams on the sky. Up to 244 beams can be formed simultaneously, making LOFAR an extremely efficient instrument to survey large areas of the sky. The Dutch part of the array will be finished in 2013 and will comprise 40 stations distributed over an area with a diameter of 100 km. In addition, the eight stations in a number of European countries (Germany, UK, Sweden, and France) are already operational. The data from the station beams are transported to the software correlator in Groningen where the initial measurements, the (raw) visibilities are made. These are discrete samples of the Fourier transform

Fig. 1 LOFAR low-band antennas optimised for the 30–80 MHz frequency range.

of the part of the radio sky that is being observed. The next step is the identification and flagging of man-made Radio Frequency Interference (RFI) resulting, for example, from radio and television stations. A major issue for low frequency radio observations is that there are several celestial radio sources so bright that they are always the dominant contribution to the interferometric signal, even if they are far away from the pointing centre. We have developed the "demixing method" which enables efficient and effective subtraction of extremely bright sources located outside the station beam (PhD van der Tol). An important advantage is that after demixing it is possible to average the data in time and frequency by a factor of typically up to 50. This has the crucial implication that a data set from a typical observing session is then less than 1 Tb and can hence be transferred over the internet. The subsequent next steps are extremely computer intensive and are described in the next sections.

2.1 Multidirectional calibration

In order to calibrate the visibilities, extensive use is made of the Measurement Equation formalism developed by Hamaker et al. (1996). The Measurement Equation provides a complete model of a generic interferometer. Each of the physical phenomena that transform or convert the electric field before the correlation performed by the correlator is modelled by linear transformations. These phenomena include the complex gain variations for all the directions of each of the antenna stations, and the impact on the polarization properties induced by the system and the ionosphere. This elegant formalism enables us to (i) model the full polarization of the visibilities as a function of the true underlying electric field correlation and (ii) to properly solve for the time and spatially varying system parameters that need to be calibrated. The collective implementation of the algorithms form the BBS (BlackBoard Selfcal) system (Pandey et al. 2009) .

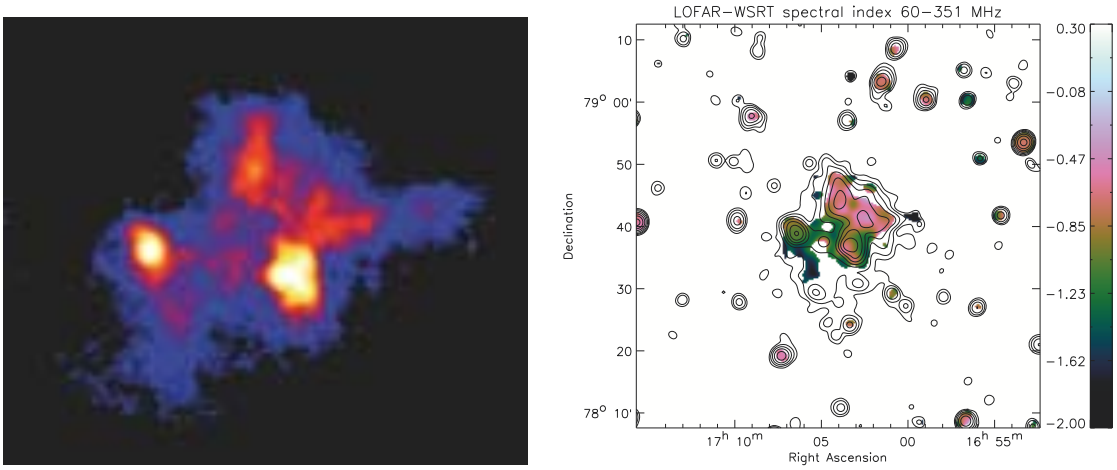

Fig. 2 *Left*: a 60 MHz LOFAR image of the rich cluster of galaxies A 2256 at $z = 0.058$ with a noise level of 10 mJy/beam and a resolution 30 arcsec. Note that only 25 stations and 4 MHz out of 48 MHz of BW was used. *Right*: a 60–351 MHz spectral index map from a combination of LOFAR and WSRT data, showing the ultra steep spectrum central radio halo and the flatter spectrum relic shock (van Weeren et al. 2012).

2.2 Ionospheric calibration

Calibration of interferometric observations at low radio frequencies is very challenging. This is mainly due to ionospheric induced phase variations that vary with time, viewing direction and antenna location (Cohen & Röttgering 2009). In the context of the PhD thesis of Huib Intema we have developed and implemented the first sophisticated ionospheric calibration method (SPAM; Intema et al. 2009). To model the ionosphere, we construct time varying two-dimensional phase screens over the array. These phase screens are described by Karhunen-Loève functions taking into account the power-law nature of the ionospheric fluctuation spectrum. This method is being implemented within the standard reduction pipeline.

2.3 Widefield imaging and deconvolution

Conceptually, the final step is a simple Fourier transform of the visibilities to obtain radio maps of the radio sky. In practice this step is extremely complicated and time consuming, particularly for the wide-field imaging that LOFAR will excel at. First, due to the large fields (and hence curvature within the image plane), a pseudo-3-d instead of a 2-d Fourier transform is needed on the already huge data sets. Second, since the sampling in Fourier space is not ideal and has – due to the maximum length baselines - sharp edges, it is essential to deconvolve the data. In close collaboration with Bhatnagar (NRAO), we have now adopted and modified his A-projection scheme for use in the LOFAR pipeline (Tasse et al. 2012). This uses convolution functions during the gridding step to reconstruct an undistorted image.

2.4 Source finding and characterization

The Leiden postdocs Mohan and Rafferty have developed PyBDSM, a software package that finds and measures the characteristics of radio sources, taking the varying angular resolution of the maps into account.

More detailed information on the reduction methods and some early science results can be found in papers by McKean et al. (2011), Mulcahy et al. (2011), Morganti et al. (2011), Röttgering et al. (2011), Heald et al. (2011), Tasse et al. (2012), van Weeren et al. (2012), Ferrari et al. (2012), and de Gasperin et al. (2012).

Although the entire software chain is complex, far from complete and not yet completely user-friendly, the first results clearly show the capability of LOFAR in making high quality astronomical observations.

At the moment the data reduction still needs development. Fortunately no significant limitations have been found that should prevent observations attaining the theoretical noise limit using 10 hour long data sets. LOFAR data on the following clusters are being analysed: Virgo cluster (de Gasperin et al., in prep.); MACS0717 (Bonafede et al., in prep.), A 2255 (Pizzo et al. in prep.), A 1682 (Macario et al., in prep.), Sausage clusters (Stroe et al., in prep.), and A 2256 (van Weeren et al. 2012, see Fig. 1).

3 Relics and halos

Clusters of galaxies are large ensembles consisting of hundreds of galaxies that are embedded in hot gas, and held together by gravity. They grow through a sequence of mergers of smaller sub-clusters. These cluster collisions are the most energetic events in the Universe after the Big Bang, releasing energies of the order of 10^{62}–10^{64} erg over timescales of a few Gyr. Radio observations of galaxy clusters have revealed the existence of large megaparsec-size, diffuse synchrotron emitting sources. They are unrelated to the radio galaxies commonly found in clusters. The observed synchrotron radiation implies the existence of highly relativistic particles (Lorentz factor $\sim 10^5$) and cluster wide mag-

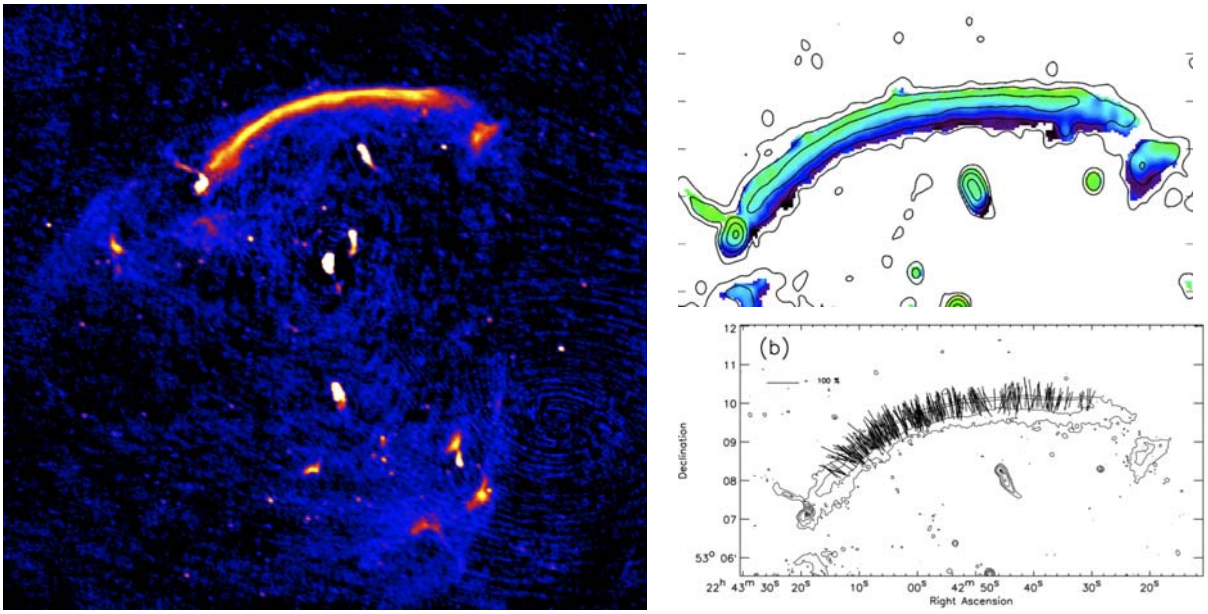

Fig. 3 *Left*: GMRT radio image at 610 MHz of the "Sausage" galaxy cluster CIZA J2242.8+5301 (redshift $z = 0.1921$). The image has an rms noise of 23 μJy beam^{-1}and a resolution of $4.8'' \times 3.9''$. Clearly visible to the north is the large 2 Mpc relic. *Upper right*: radio spectral index map of the Sausage relic, determined using matched observations at 2.3, 1.7, 1.4, 1.2, and 0.61 GHz, fitting a power-law radio spectrum to the flux density measurements. The relic displays a strong spectral index gradient ranging from $\alpha = -0.6$ down to $\alpha = -2.0$ towards the center of the cluster due to cooling of the synchrotron emitting particles in the post-shock region. *Lower right*: map of the the polarization electric field vector obtained with the VLA at a frequency of 4.9 GHz. The vectors were corrected for the effects of Faraday rotation using a Faraday depth of -140 rad m^{-2} determined from WSRT observations at 1.2 to 1.8 GHz (from van Weeren et al. 2010).

netic fields ($\sim \mu$Gauss). LOFAR is uniquely suited to probe these synchrotron emitting regions and will address many questions related to the large-scale magnetic fields and relativistic particles mixed with the thermal ICM. These questions include: What are the strengths and topologies of the magnetic fields? How are the magnetic fields generated and maintained? How do the merging clusters induce particle acceleration?

Diffuse radio emission associated with clusters of galaxies has been classified into two main groups: relics and halos (e.g. Feretti et al. 2012).

Cluster relics are large elongated diffuse structures at the periphery of clusters. Often they are highly polarised. *Cluster radio halos* are located at the centres of clusters, their diffuse morphologies following that of the X-ray emission. The fraction of clusters with a radio halo increases with cluster mass with the fraction of clusters hosting halos being 0.3 for the most massive systems (Cassano et al. 2011).

3.1 Sausage cluster

Recently we have discovered a spectacularly long and narrow relic with a size of 1.7 Mpc$\times$50 kpc, located at a distance of $\sim$1.5 Mpc from the centre of the merging cluster CIZA J2242.8+5301 at a redshift of $z = 0.19$ (van Weeren et al. 2010; Stoe et al. 2012 in prep.; Fig. 3). The overall morphology led us to nickname the cluster the "Sausage cluster". The relic displays a strong spectral index gradient and a highly ordered magnetic field. The proposed scenario is a massive merger shocks created outwards shocks. At the front of the shock particles are accelerated to such high energies that they start radiating synchrotron emission. The spectral index at the front of the shock indicates that the Mach number of the outgoing main shock is of order of $M = 4$. In the downstream area the electrons lose energy due to synchrotron and inverse Compton interactions, resulting in the observed strong spectral index gradient. The observed high polarisation fraction of the emission indicates that the shock has well-ordered magnetic field lines (see Fig. 3). From a further analysis of the radio properties, we deduce that the magnetic field strength is 5 μG. We have carried out extensive numerical simulations of this cluster, coupling hydrodynamic gas simulations with a method to predict radio emission from shocks (van Weeren et al. 2011). On the basis of these simulations we have shown that a consistent set of parameters describing the merging event can be determined. These parameters include: mass ratio of merging clusters (1:2), impact parameter ($<$500 kpc), orientation (within 10 degrees on the plane of the sky), and time since core passage (0.1 Gyr).

3.2 Toothbrush cluster

Recently we have discovered the cluster 1RXS J0603.3 +4214 ($z = 0.225$) and found that it hosts a large bright

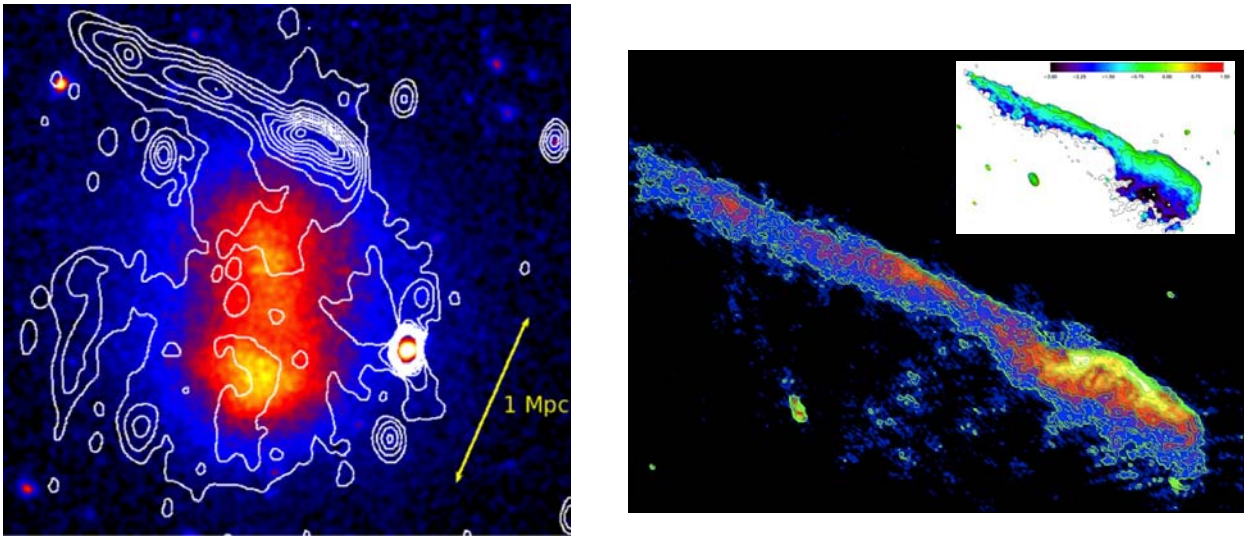

Fig. 4 *Left*: the XMM-*Newton* 0.5–4 keV image of the Toothbrush cluster overlaid with the WSRT 1.4 GHz radio contours (*right*). The GMRT 1.2 GHz image. Inserted is the GMRT 610–325 MHz spectral index map, showing that the relic displays a strong spectral index gradient from $\alpha = -0.6$ down to $\alpha = -2.0$ towards the center of the cluster (from van Weeren et al. 2012).

1.9 Mpc radio relic, an elongated 2 Mpc radio halo, and two fainter smaller radio relics (van Weeren et al. 2012, see Fig. 4). The large radio relic has a spectacular linear morphology and a clear spectral index gradient from the front of the relic towards the back, in the direction towards the cluster center. Parts of this relic are highly polarized with a polarization fraction of up to 60 %. The XMM-*Newton* observations clearly show a violent cluster-cluster merging event (Fig. 4). As double mergers naturally give rise to curved traveling shock fronts, the linear morphology is puzzling. A way to explain this morphology is to invoke a triple merger event. Brüggen et al. (2012) carried out hydrodynamical N-body AMR simulations of a number of triple merger events. A scenario that resulted in a 2 Mpc linear shock started with two equal mass clusters with an an initial relative velocity of 1500 km s^{-1} whose cores collide 1.3 Gyr after the start of the simulation. Before core passage a less massive third cluster grazes the southern cluster and loses some of its gas and dark matter. As it then heads north, this third cluster drives a second major shock into the ICM that merges with the previous shock to form a fairly plane shock front. In projection this shock front has a morphology similar to the Toothbrush relic.

Acknowledgements. C. Ferrari and G. Macario acknowledge financial support by the "Agence Nationale de la Recherche" through grant ANR-09-JCJC-0001-01. R. van Weeren was supported for this work by NASA through Einstein Postdoctoral grant number PF2-130104 awarded by the Chandra X-ray Center, which is operated by the Smithsonian Astrophysical Observatory for NASA under contract NAS8-03060.

References

Brüggen, M., van Weeren, R. J., & Röttgering, H. J. A. 2012, MNRAS, 425, L76
Cassano, R., Brunetti, G., & Venturi, T. 2011, JA&A, 32, 519
Cohen, A. S., & Röttgering, H. J. A. 2009, AJ, 138, 439
de Gasperin, F., Orrú, E., Murgia, M., et al. 2012, A&A, 547, A56
Ferrari, C., van Bemmel, I., Bonafede, A., et al. 2012, First LOFAR results on galaxy clusters, in SF2A-2012, ed. S. Boissier, P. de Laverny, N. Nardetto, R. Samadi, D. Valls-Gabaud, & H. Wozniak (Société Francaise d'Astronomie et d'Astrophysique), 677
Hamaker, J. P., Bregman, J. D., & Sault, R. J. 1996, A&AS, 117, 137
Heald, G., Bell, M. R., Horneffer, A., et al. 2011, JA&A, 32, 589
Intema, H. T., van der Tol, S., Cotton, W. D., et al. 2009, A&A, 501, 1185
McKean, J., Ker, L., van Weeren, R. J., et al. 2011, astro-ph/1106.1041
Morganti, R., Heald, G., Hessels, J., et al. 2011, astro-ph/1112.5094
Mulcahy, D. D., Drzazga, R., Adebahr, B., et al. 2011, astro-ph/1112.1300
Ogrean, G., Brüggen, M., Röttgering, H., et al. 2013, MNRAS, 429, 2617
Pandey, V. N., van Zwieten, J. E., de Bruyn, A. G., & Nijboer, R. 2009, Calibrating LOFAR using the Black Board Selfcal System, in The Low-Frequency Radio Universe, ed. D. J. Saikia, D. A. Green, Y. Gupta, & T. Venturi, ASPC 407, (ASP, San Francisco), 384
Röttgering, H., Afonso, J., Barthel, P., et al. 2011, JA&A, 32, 557
Tasse, C., van Diepen, G., van der Tol, S., et al. 2012, Comptes Rendus Physique, 13, 28
van Weeren, R. J., Röttgering, H. J. A., Brüggen, M., & Hoeft, M. 2010, Sci, 330, 347
van Weeren, R. J., Brüggen, M., Röttgering, H. J. A., & Hoeft, M. 2011, MNRAS, 418, 230
van Weeren, R. J., Röttgering, H. J. A., Intema, H. T., et al. 2012a, A&A, 546, A124
van Weeren, R. J., Röttgering, H. J. A., Rafferty, D. A., et al. 2012b, A&A, 543, A43